Journal of
Materials Chemistry A

Accepted Manuscript

This article can be cited before page numbers have been issued, to do this please use: Q. Liu, B. Jin, R. Peng, Z. Guo, J. Zhao, Q. Zhang and Y. Shang, *J. Mater. Chem. A*, 2016, DOI: 10.1039/C5TA10688E.

ROYAL SOCIETY OF CHEMISTRY

www.rsc.org/materialsA

Synthesis, Characterization and Properties of Nitrogen-rich Compounds based on Cyanuric Acid: A Promising Design in the Development of New Energetic Materials

Qiangqiang Liu[a,b], Bo Jin[a]*, Rufang Peng[a,b]*, Zhicheng Guo[c], Jun Zhao[a], Qingchun Zhang[a], Yu Shang[a]

[a] State Key Laboratory Cultivation Base for Nonmetal Composites and Functional Materials, Southwest University of Science and Technology, Mianyang 621010, China

[b] Research Center of Laser Fusion, China Academy of Engineering Physics, Mianyang, 621010, China

[c] School of Nation Defence Science and Technology, Southwest University of Science and Technology, Mianyang 621010, China

Abstract: Nitrogen-rich compounds such as ammonium (**1**), hydrazinium (**2**), aminoguanidinium (**3**), diaminoguanidinium (**4**), triaminoguanidinium (**5**), aminonitroguanidinium (**6**), aminocarbonylguanidinium (**7**), metforminium (**8**), based on nitrogen-rich anion [CA^- (N % = 32.55%, CA= Cyanuric Acid) and co crystal 5-amino-1*H*-tetrazole based on CA (**9**) were synthesized by means of metathesis reactions. The crystal structures of compounds **2**, **4**, and **9**·H_2O were determined by single-crystal X-ray diffraction and fully characterized by UV-Vis, FT-IR, ^{1}H NMR, MS and elemental analysis. The thermal stabilities were investigated by differential thermal analysis (DTA) and thermo gravimetric analysis (TGA). The DTA results show that all compounds exhibit high thermal stabilities. Additionally, the heats of formation were calculated by using the B3LYP functional with 6-311++G** basis set and a Born–Haber energy cycle. Theoretical calculations provided detonation pressures and velocities for the energetic salts within the range of 16.88-30.71 GPa and 6276.5-8392.1 m/s, respectively. Impact sensitivities of the compounds were determined by the Fall hammer test. All compounds show insensitive impact sensitivities (＞ 60 J), which are better than that of TATB (50 J).

Key words: Nitrogen heterocycles, Nitrogen-rich compounds, Thermal stabilities, Detonation properties

Introduction

As a significant branch of material science, energetic materials including explosives, propellants, and pyrotechnics, continue to be an intensively investigated area of the utmost importance. High energy density materials (HEDMs) have become the frontier of energetic material development, which are one of the most important key technologies of national defense and have been given unprecedented attention by many countries. High-nitrogen heterocycles represent a unique class of energetic molecules, which have recently attracted significant interest in the fields of energetic materials. Five- or six-membered nitrogen-rich heterocyclic compounds, such as triazole[1-4], tetrazole[5-7], triazine[8-11], and tetrazine[12-14], have been investigated extensively to screen for promising candidates for HEDMs[15-30].

1,3,5-Triazines (or *s*-triazines) rings have been studied for use in a number of applications such as herbicides, synthesis, dyes, and polymers[31-35]. *s*-Triazines and its derivatives such as melamine represent an important class of industrial chemicals, and the theoretical and experimental researches on triazine and its derivatives have been very active[8, 36-40]. A series of derivatives of 1,3,5-triazines containing energetic substituent (like azido, nitamino or nitro) were investigated (Figure 1 a), owing to their positive heat of formation, high nitrogen content, and thermal stability[41, 42]. Although these compounds are highly energetic due to their positive heats of formation, the characteristics of high sensitivity significantly limit their application potential for use on a large scale (Figure 1 b).

In the last decade, a unique class of high energetic compounds composed of nitrogen-containing heterocyclic anions and/or cations have been developed to meet the continuing demand for improved energetic materials[10, 43-47]. Nitrogen-rich ionic salts have constituted a unique class of energetic materials and attracted substantial interests due to their "greenness" of explosion products, toxicity to human health, intrinsically low volatility, low vapor pressure, low handling hazards, high thermal stability, simple synthesis routes for low cost etc[48-60]. Because of its low tension, good stability, high nitrogen content (51.83%), and higher formation enthalpy, 1,3,5-triazine, a six-membered ring heterocycle with alternating C-N bonds, is a potential building block for emerging energetic compounds. As the most ubiquitous triazines, melamine and cyanuric chloride are usually used as substrate in synthesis of *s*-triazine-based energetic salts[8,85]. There are scarcely reports on cyanuric acid (CA) as raw material. Herein, we present our attempts at designing and synthesizing a series of high-nitrogen triazine-salts compounds through the strategy of bonding an energetic cation and the CA anion. For these new ionic salts, the high nitrogen content of both the cations and anions are expected to contribute higher crystal density, higher heats of formation, and environmentally benign decomposition products (N_2), and thereby result in an excellent detonation

performance. The compounds shows outstanding thermal stability, good detonation properties and insensitive impact sensitivities, which suggest that they are insensitive energetic materials.

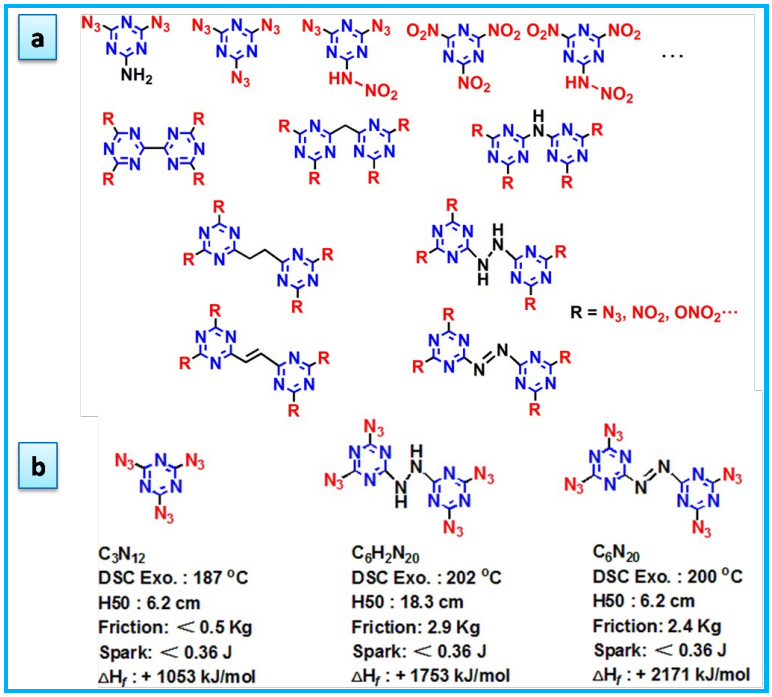

Figure 1 Molecular frameworks (a) and properties (b) of derivatives of 1,3,5-triazines

Results and Discussion

Syntheses

As shown in scheme 1, a series of triazine-salts and co crystal based on CA were synthesized and their structures were fully investigated and confirmed by UV-Vis, IR spectroscopy, ^{1}H NMR, ^{13}C NMR, mass spectrometry and elemental analyses. All the products were stable in air and could be stored for months.

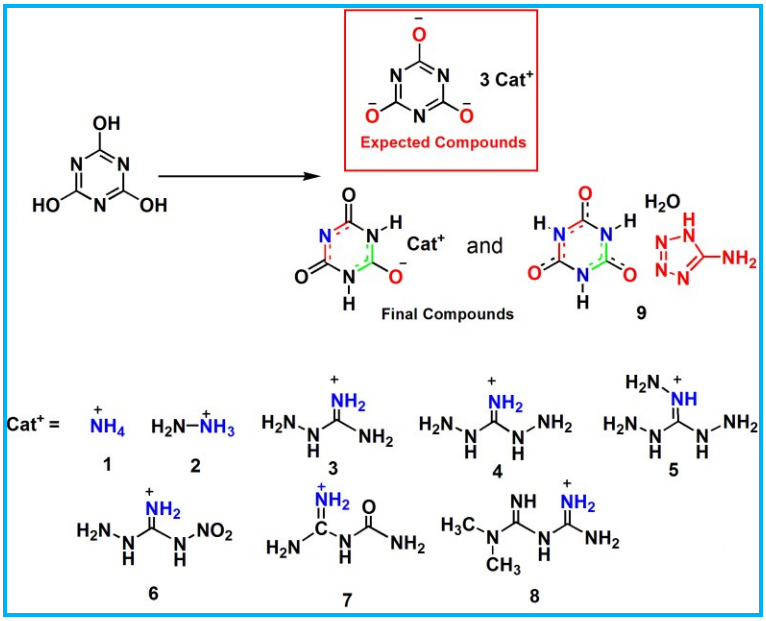

Scheme 1 Syntheses of the CA salts and co crystal

In this work, our expected compounds should be a maximum of three cations in each salt (Scheme 1 Expected Compounds). However, all characterizations (i.e. X ray single crystal diffraction, mass spectrometry, elemental analysis) indicated that 1:1 stoichiometry compounds were obtained (As shown in Scheme 1 Final Compounds). Ammonium 4,6-dione-3,5-dihydro-[1,3,5]triazin-2-ol **(1)** and hydrazinium 4,6-dione-3,5-dihydro-[1,3,5]triazin-2-ol **(2)** were prepared by the selective action of CA with aqueous ammonia and hydrazine hydrate (80%) at room temperature, respectively. Barium based on CA was treated directly with aminoguanidine sulfate and guanylurea sulfate in water to form

aminoguanidinium **(3)** and aminocarbonylguanidinium **(7)** in excellent yields. Organic hydrochloride reacted with sodium salts or silver salts of CA to achieve the products **4, 5, 6** and **8**. Herein, the same products were obtained when diaminoguanidinium hydrochloride, triaminoguanidinium hydrochloride, aminonitroguanidinium hydrochloride, and metforminium hydrochloride reacted with sodium salt and silver salt.

View Article Online
DOI: 10.1039/C5TA10688E

It is interested and unexpected that **9** can be get by reacting CA-anion with 5-amino-1*H*-tetrazole or its hydrochloride, and its exothermic peak is higher than 400 °C. It has a total mass loss 69.1% after heating up to 850 °C. At the same time, the single crystal of compound **9** was obtained and characterized, which was used to compare with other products (i.e. **2** and **4**) and explain this interesting phenomenon.

Crystal Structures

Crystals of **2, 4,** and **9** suitable for single-crystal X-ray diffraction were cultured by slow evaporation of the respective solvent at room temperature and normal pressure. Their crystallographic and structural refinement data are summarized in Table 1, and structures are shown in Figures 2-7, respectively. Further information about crystal-structure determinations is given in the Supporting Information.

Table 1. Crystallographic data and structure refinement parameters.

	2	**4**	**9**·H_2O
Formula	$C_3H_7N_5O_3$	$C_4H_{10}N_8O_3$	$C_4H_7N_8O_4$
M(g/mol)	161.14	218.17	232.18
Crystal Color	colorless	colorless	colorless
Crystal System	Monoclinic	Triclinic	Triclinic
Space Group	*P*2(1)/n	*P*-1	*P*-1
a [Å]	9.4591(15)	6.7212(17)	5.4748(11)
b [Å]	6.7214(10)	11.023(3)	9.655(2)
c [Å]	9.6711(15)	11.825(3)	9.881(2)
α [°]	90	87.770(9)	66.29(2)
β [°]	101.349(3)	82.156(8)	75.35(3)
γ [°]	90	78.806(7)	72.33(3)
V [Å^3]	602.85(16)	851.3(4)	450.50(19)
Z	4	4	2
T [k]	113	113	113
λ [Å]	0.71073	0.71075	0.71075
ρ_{calcd} [g/cm-3]	1.775	1.702	1.712
μ [mm^{-1}]	0.156	0.144	0.150
F (000)	336	456	238
crystal size [mm^3]	0.240×0.220×0.180	0.260×0.240×0.220	0.260×0.240×0.220
θ_{max} [°]	27.506	35.022	27.483
No. Refl. collected	5845	14660	5846
No. Indep. reflections	1380	7145	2036
[R_{int}]	0.0228	0.0174	0.0800
GOF[a] on F^2	1.056	1.064	1.068
R_1 [b] [$I>2\sigma(I)$]	0.0254	0.0338	0.0746
wR_2 [c] [All refl.]	0.0792	0.1059	0.2233
CCDC number	1435469	1410778	1410779

[a]GOF= Goodness of Fit; [b] $R_1 = \sum||F_o|-|F_c||/\sum|F_o|$ [c] $wR_2 = [(w(F_o^2-F_c^2)^2)/w(F_o^2)^2]^{1/2}$

The X-ray crystallographic analysis data for **2** shows that it crystallizes in the monoclinic space group $P2_1/n$ with a calculated density of 1.775 g/cm^3 (Figures 2) based on four molecules packed in the unit-cell volume of 602.85(16) Å^3 (Table 1). Compared with the structure of CA·H_2O (Figure S1), all the C-N bonds and C-O bonds are slightly changed (C-N bond length from 1.374 Å to 1.383 Å, C-O bond lengths 1.225 Å), which may be caused by the negative charge on anion

rings. The bond lengths of C1-N1 [1.3528(11) Å], C1-N2 [1.3903(11) Å], C2-N2 [1.3657(12) Å], C2-N3 [1.3651(11) Å], C3-N3 [1.3872(11) Å] and C3-N1 [1.3437(12) Å] are between standard C–N single bond (1.47 Å) and standard C=N double bond (1.32 Å) lengths and indicative of an aromatic system[61, 62]. The C1-O1, C2-O2 and C3-O3 bond lengths (approx. 1.24 Å) are longer than the standard C=O [1.215 Å] double bond[63], indicating the CA-anion ring tautomerism. In addition, the bond angles of nitrogen heterocyclic in the range of 114.53(7)- 123.44(7) ° are closed to 120 °, which further confirm tautomerism of *s*-triazines ring. Meanwhile, all the torsion angles [i.e. C3-N1-C1-O1(-178.08 °), C1-N-C3-N3(1.11 °)] are close to ±180 ° and 0 °, which illustrates atoms of anion are strictly coplanar. If there are no symmetry transformations used to generate equivalent atoms, each molecule has only one hydrogen bond N(2)-H(2)...N(5), and strong hydrogen bond interaction makes the bond length of N2-H2 [0.924(14) Å] slightly longer than that of N3-H3 [0.882(16) Å]. However, there are many intermolecular hydrogen bonds in compound **2**, and its packing diagram shows that it is cross layered stacking structure viewed down the b axis (Figure 3). Layers are connected by many hydrogen bonds, which exist between 1,3,5-triazines rings and hydrazine cations, and there are hydrogen bonds in configuration similar two layer.

View Article Online
DOI: 10.1039/C5TA10688E

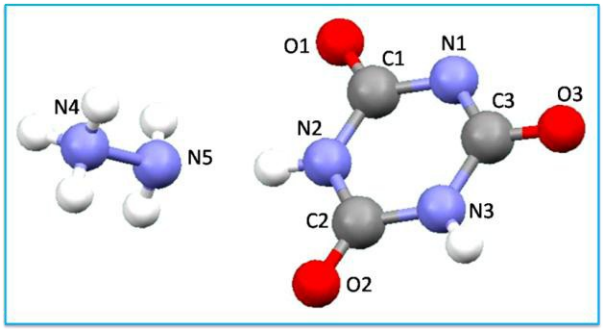

Figure 2 Ball-and-stick molecular structure of **2**.

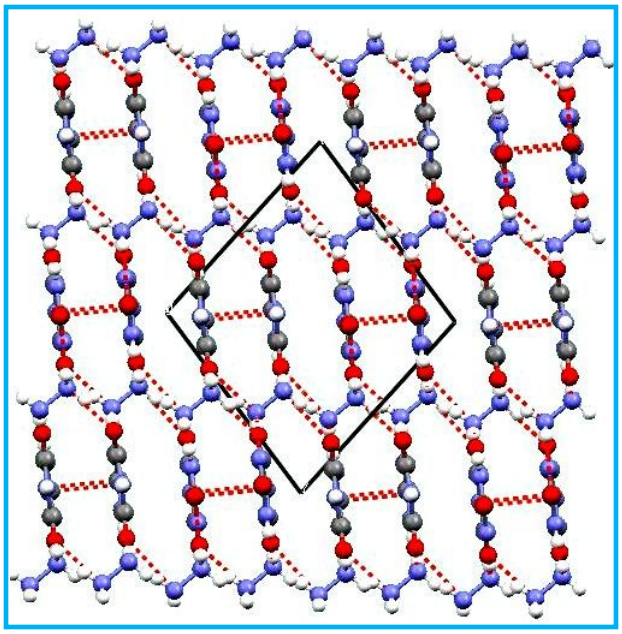

Figure 3 Ball-and-stick packing diagram of **2** viewed down the b axis. Dashed lines indicate hydrogen bonding.

Crystal of the diaminoguanidinium 4,6-dione-3,5-dihydro-[1,3,5]triazin-2-ol **(4)** depicted in Figure 4 and crystallizes in the triclinic space group *P*-1 with two diaminoguanidinium cations and two CA-anions in the unit cell. The density of salt **4** is 1.702 g/cm^3 and the cell volume is 851.3(4) Å^3, which is larger than compound **2**. In contrast to the crystal structure of **2**, the triazine anion moiety in product **4** is not planar and the density is slightly lower than that of **2**. There are a little change in bond lengths of C-N, and these are also between standard C–N single bond and standard C=N double bond lengths. All the C-O bonds lengths are similar to that of compound **2** except C2-O2 and C4-O4 bond lengths. In salt **2**, the position of hydrazinium cations are close to hydrogen atom between C1-O1 and C2-O2, however, the diaminoguanidinium cations of **4** are near to oxygen atom not to hydrogen atom. So, C2-O2 and C4-O4 bond lengths become a little bit longer.

The anion bond angles of salt **2** and salt **4** are almost the same . Compared with compound **2**, salt **4** have three kinds of hydrogen bonds, one is the hydrogen bonds between anions and cations, another one is the hydrogen bonds formed by anions to anions, the other one is cations to cations. Its packing structure is configured by hydrogen bonds; the extensive

hydrogen-bonding interactions form a complex 3D network (Figure 5). Further details are provided in the Supporting Information.

View Article Online
DOI: 10.1039/C5TA10688E

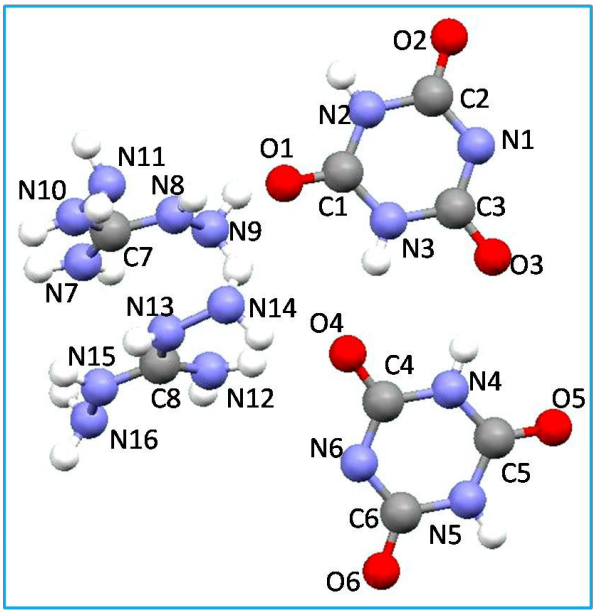

Figure 4 Ball-and-stick molecular structure of **4**.

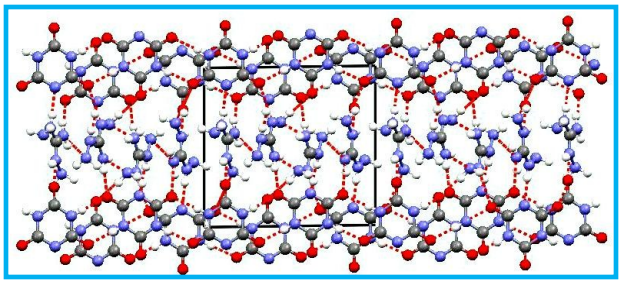

Figure 5 Ball-and-stick packing diagram of **4** viewed down the a axis. Dashed lines indicate hydrogen bonding.

Compound **9**·H_2O crystallizes in the monoclinic pace group *P*-1 with two molecular units in the unit cell, a cell volume of 450.50(19) $Å^3$, which is smaller than any other's volume, and a density of 1.712 g/cm^3, which is slightly higher than that of CA monohydrate (1.682 g/cm^3) and similar to 5-amino-1*H*-tetrazole monohydrate (1.711 g/cm^3). As shown in Figure 6, the unit contains one independent molecule of **9** and a co-crystallized solvent molecule of H_2O. In contrast to other salts, the bond lengths of C1-O1 [1.229(4) Å], C2-O2 [1.227(3) Å] and C3-O3 [1.223(3) Å] are very close to each other and longer than the standard C=O [1.215 Å] double bond, which caused by *s*-triazines ring tautomerism. Another reason is that it is co crystal rather than ionic salt. The bond lengths of N5=N6 [1.360(4)Å], N6=N7 [1.290(3)Å], and N7=N8 [1.356(4)Å] are slightly longer than that of typical N=N double bonds (1.245 Å)[12], and C-N bond lengths [i.e. C1-N1(Å), C1-N3(1.371Å), C2-N2(1.367Å), C3-N2(1.371Å), C4-N5(1.334Å), C4-N8(1.335Å)] are also between standard C–N single bond and standard C=N double bond lengths. All of these indicate that the conjugated structures are existed in both tetrazole and triazine rings. The torsion angles of compound **9**, such as C1-N1-C2-O2 [-177.7(2) °], C2-N2-C3-O3 [179.98(19) °], C2-N2-C3-N3 [-0.9(3) °], C3-N2-C2-O2 [-179.35(19) °], N6-N5-C4-N4 [178.18(19) °], C4-N5-N6-N7 [0.1(2) °], N7-N8-C4-N4 [-178.26(19) °] , are close to 0 °or ±180 ° which support that all atoms are coplanar except hydrogen on the water molecules and primary amines. As shown in Figure 7(a), the hydrogen bonds are observed in the packing diagram, which are gathered in the Supporting Information. Compared with other salts, **9** have five kinds of hydrogen bonds, and they are the hydrogen bonds between *s*-triazines rings and 5-amino-1*H*-tetrazole rings, and hydrogen bonds formed by triazines rings to triazines rings, tetrazole rings to tetrazole rings, and triazines rings or tetrazole rings to H_2O. Two *s*-triazines rings and two tetrazole rings are connected by two water molecules with strong hydrogen bond interactions. Because of hydrogen bonds, N-H and O-H bond lengths become longer than that of CA·H_2O [i.e. N1-H1 0.98(4) Å to 1.05(3) Å, N3-H2 0.85(4) Å to 0.88(3) Å , O-H in H_2O 0.92(5) Å to 1.05(3) Å], and bond angle of crystallization water increase from 106(3) °to 116(4) °. Compound **9** is roughly parallel layer-to-layer structure, and there are no hydrogen bond among each layer (Figure7 b).

View Article Online
DOI: 10.1039/C5TA10688E

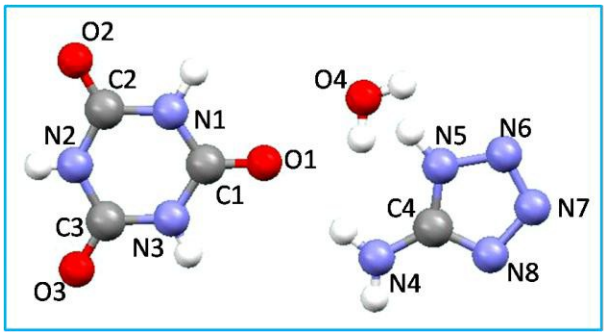

Figure 6 Ball-and-stick molecular structure of **9**·H_2O.

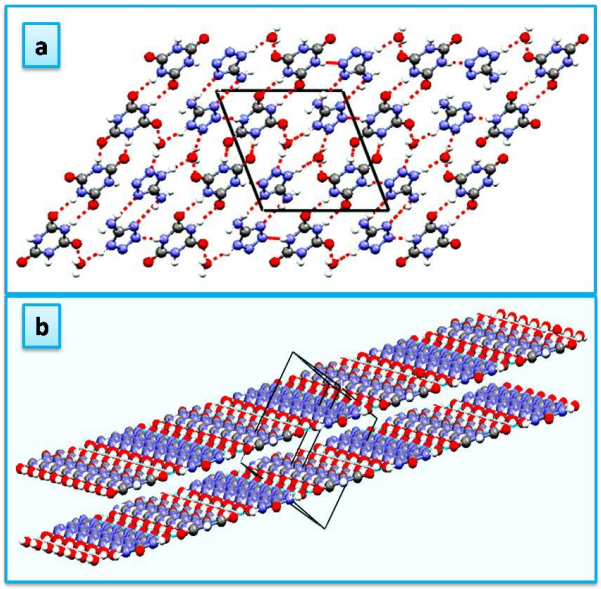

Figure 7 Ball-and-stick packing diagram of **9**·H_2O viewed down the a axis(a), layer-to-layer structure of 9(b). Dashed lines indicate hydrogen bonding.

Thermal Behavior

In order to determine the melting points and decomposition temperatures approx. 3.0 mg of each material were measured by differential thermal analysis (DTA) in open crucible at a heating rate of 10 °C/min with static air atmosphere. As shown in Table 2, only salts **3** and **4** have melting at 280.0 and 252.3 °C, respectively, and higher than that of TNT (80.4 °C) and RDX (204.1 °C). The decomposition temperature (T_d) of all compounds is higher than RDX (230.0 °C) except compound **2** and **6**, and some compounds (**1**,**9**·H_2O) even higher than that of TNT (295.0 °C). T_d of all products, in the range of 192.8 °C (**2**) to 417.5 °C (**9**·H_2O), indicate that these compounds are promising energetic materials that exhibit good thermal stability.

Table 2 Thermal properties of compounds **1-9**

	1	**2**	**3**	**4**	**5**	**6**	**7**	**8**	**9**·H_2O	**TNT**[c]	**RDX**[c]
T_m[a]/°C	—	—	280.0	252.3	—	—	—	—	—	80.4	204.1
T_{dec}[b]/°C	364.2	192.8	292.8	255.2	253.2	202.1	248	238.5	417.5	295.0	230.0

[a] Melting point["—"means no melting points]. [b] Decomposition peak temperature.[c] Reference [64]

In this work, decomposition process of compounds **2, 4, 5, 6** and **9**·H_2O were also investigated by thermo gravimetric analysis (TGA) at a heating rate 10 °C/min with air atmosphere. As shown in Figure 8, salts **2, 4, 5** and **6** have three steps decomposition to be cations, anionic skeletons and fragments, and when heated to 600 °C the whole mass loss are up to 99.2%, 99.8%, 99.0% and 99.5%, respectively.

View Article Online
DOI: 10.1039/C5TA10688E

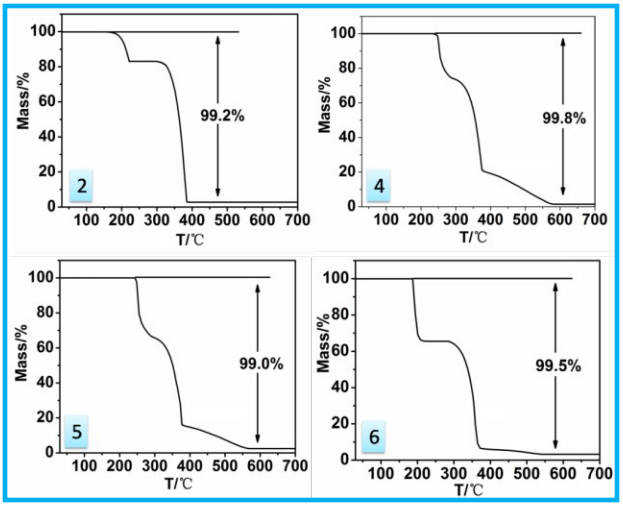

Figure 8 TG curves of salts **2,4,5** and **6** under air atmosphere

It is interested and unexpected that **9** is a co-crystal of CA and 5-amino-1*H*-tetrazole. The TG and DTG curves (Figure 9) show that it has a total mass loss 69.1% with four step decomposition until the temperature up to 850 °C. First step, crystal water of 9 begins to lose weight at 183.5 °C, and the mass loss is 10.77% and DTG peak temperature at 190.8 °C (endothermic). Second and third steps have 50.12% mass loss due to heterocyclic skeleton decomposition. The onset temperature is 397.3 °C and peak temperatures are 415.5 °C (endothermic) and 444.0 °C (exothermic), respectively. The last step is decomposition of small pieces which produced by heterocyclic skeleton decomposition at 751.4 °C (exothermic). The characteristics (composition, morphology, microstructure and so on) of the residue (about 30%) after heating up to 850 °C need to be further investigated.

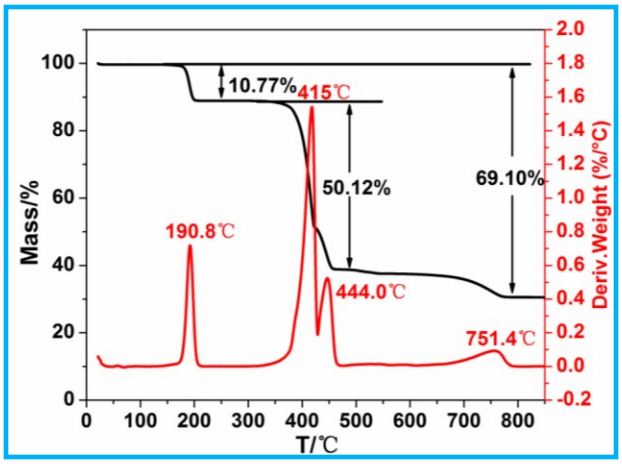

Figure 9 TG and DTG curves of co-crystal **9** under air atmosphere

Energetic Properties

The heat of formation (HOF) is an important parameter in evaluating the performance of energetic salts, which can be calculated with good accuracy (including the heat of formation of the cations and anion and the lattice energy of salts) [19, 20, 65-67]. The HOF of the anion based on isodesmic reaction (Scheme 3) was calculated to be -66.4 kJ/mol; the values for the cations are available in the literature[64, 68]. As summarized in Table 3, the positive heat of formation of salts **2**–**6** were calculated using the Born–Haber energy cycle. HOFs of the salts were in the range of 118.9 kJ/mol (**3**) to 337.5 kJ/mol (**5**), which is much higher than that of HMX (104.8 kJ/mol), TNT (95.3 kJ/mol) and RDX (83.8 kJ/mol).

Oxygen balance (OB), an expression used to indicate the degree to which an explosive can be oxidized, is an important index for identifying the potential of energetic materials as explosives or oxidants. It is a shortage that all salts have negative oxygen balance, which fell in the range of -44.61% (**5**) to -19.35% (**6**), and only oxygen balance of **6** is slightly better than that of TNT (-24.67%) and RDX (-21.61%) . In addition, all these salts have high nitrogen-oxygen content, most of them exceeding 70%, especially **6** reaching as high as 77.39%, which conform with its good oxygen balance.

The performance of a high explosive is characterized by its detonation velocity, *v*D [m/s], and detonation pressure, P [GPa]. The empirical Kamlet–Jacobs equations (shown as equation 4 and 5) were employed to estimate the values of detonation velocity and detonation pressure. As shown in Table 3, the detonation pressures of salts **2**–**6** ranged from 16.88

GPa (**3**) to 30.71 GPa (**6**). Salt **3** exhibited the lowest value 16.19 GPa, which is lower than that of TNT (19.5 GPa). The values of other salts are all higher than that of TNT, especially salts **6**, with the values 30.71 GPa. The detonation velocities of these salts are distributed from 6276.5 m/s (**3**) to 8392.1 m/s (**6**), and salt **3** also displayed the lowest value, lower than that of TNT (6881 m/s). The values of other salts were all above that of TNT, especially salts **2** (8328 m/s) and **6** (8392 m/s), higher than TATB (8114 m/s). For most of them are superior to TNT, thus the investigated compound may be of interest as potential energetic materials.

View Article Online
DOI: 10.1039/C5TA10688E

Sensitivity deserves significant attention by researchers because it is closely linked with the safety of handling and applying explosives. In this study, impact sensitivities of the compounds were determined using the fall hammer test with approximately 50 mg samples (5.0 kg drop hammer), and found that the impact sensitivities were more than 60 J, which are listed in Table 3. Salts of **2-6** are less sensitive to impact, which is possibly caused by the tautomerism of *s*-triazines ring to strengthen the bonds in the anions. In other words, the formation of salts greatly reduces the sensitivities. Co crystal **9**·H_2O is also an insensitive compound, which may be caused by the tautomerism of *s*-triazines ring and strong hydrogen bonds formed among triazines rings, tetrazole rings and crystal water. The impact sensitivities of all compounds are more insensitive than that of RDX (7.4 J), HMX (7 J) and TNT (15 J), even better than that of TATB (50 J). As is the case for the very insensitive explosive TATB, these compounds can significantly improve the safety and survivability of munitions, weapons, and personnel, in addition to their quality explosive properties.

Table 3 Properties of compounds **2-6** and **9**·H_2O compared with TNT/RDX/TATB

	ρ[a] [g/cm^3]	N[b] [%]	OB[c] [%]	$\Delta_f H_{cation}$[d] [kJ/mol]	$\Delta_f H_{anion}$[e] [kJ/mol]	ΔH_L[f] [kJ/mol]	$\Delta_f H_{salt}$[g] [kJ/mol]/[kJ/g]	P[h] [GPa]	vD[i] [m/s]	IS[m] [J]
2	1.775	43.47	-34.77	774.1	-66.4	535.5	172.2/1.07	30.51	8328.0	>60
3	1.70	48.26	-43.33	671.6	-66.4	486.3	118.9/0.59	16.88	6276.5	>60
4	1.702	51.54	-44.01	772.7	-66.4	489.2	217.3/1.0	26.04	7794.5	>60
5	1.70	54.72	-44.61	875.1	-66.4	480.8	327.9/1.41	27.31	7984.8	>60
6	1.75	42.41	-19.35	877.0	-66.4	473.1	337.5/1.36	30.71	8392.1	>60
9·H_2O	1.704	49.54[k]	-26.28[k]	—	—	—	172.4/0.74[l]	25.89	7757.3	>60
TNT[j]	1.648	18.50	-24.67	—	—	—	95.3/0.42	19.5	6881	15
RDX[j]	1.806	37.84	-21.61	—	—	—	83.8/0.38	34.9	8748	7.4
TATB[n]	1.86	32.55	-18.60	—	—	—	-139.7/-0.54	31.15	8114	50

[a] Calculated density. Density of **3** and **5** were taking the density of **4** as a reference. [b] Nitrogen and Oxygen content. [c] CO oxygen balance (OB) is an index of the deficiency or excess of oxygen in a compound required to convert all C into CO and all H into H_2O. For a compound with the molecular formula of $C_aH_bN_cO_d$ (without crystal water), OB[%] = 1600 [(d-a-b/2)/M_w]. [d] Molar enthalpy for the formation of the cations, Reference[68]. [e] Calculated molar enthalpy for the formation of the anion. [f] The lattice energy of the ionic salts. [g] Calculated molar enthalpy for the formation of the salts. [h] Detonation pressure. [i] Detonation velocity. [j] Reference[64] [k] Calculated without crystal water. [l] the heat of formation for the compound iscalculated by addition of $\Delta_f H^\circ$(s, 298K) for H_2O, which is -311kJ/mol. [m] Impact sensitivity. [n] Reference[43,83,84].

Conclusions

A family of nitrogen-rich compounds based on ammonium (**1**), hydrazinium (**2**), aminoguanidinium (**3**), diaminoguanidinium (**4**), triaminoguanidinium (**5**), aminonitroguanidine (**6**), aminocarbonylguanidinium(**7**), metforminium (**8**) and 5-amino-1*H*-tetrazole (**9**) combined with CA-anion or CA were prepared and fully characterized by IR and ^{1}H NMR spectrum, DTA, and elemental analysis. The structures of **2, 4** and **9** were also analyzed by single-crystal X-ray diffraction. All the compounds exhibited excellent thermal stabilities (192.7 to 417.5 ^{o}C), and the density range from 1.702 g/cm^3 (**4**) to 1.775 g/cm^3 (**2**). In addition, the detonation properties were calculated and most salts exhibited good detonation velocities (the best 8392.1 m/s) and detonation pressure (the best 30.71 GPa). More important, BAM fall hammer tests show that these compounds are very insensitive (IS > 60 J) to impact. Depending on the good detonation properties, excellent impact sensitivities and high thermal stabilities, these compounds have intensively potential application for energetic materials. In

brief, the CA and its derivatives were proved to be an excellent backbone of novel energetic salts.

Experimental Section

View Article Online
DOI: 10.1039/C5TA10688E

Caution: Although none of the compounds described here has exploded or detonated in the course of this research, these materials should be handled with extreme care by using the best safety practices.

X-ray analyses: Clear prism crystals of **2, 4** and **9** were mounted on mounted on a glass fiber. All measurements were made on a Rigaku XtaLAB P200 diffractometer using multi-layer mirror monochromated Mo-Kα radiation. All calculations were performed using the Crystal Structure[69] crystallographic software package except for refinement, which was performed using SHELXL2014[70].

Computational details: Computations were performed with the Gaussian 09 program[71]. The geometric optimization of the structures based on single-crystal structures, where available, and frequency analyses were carried out by using the B3LYP functional with 6-311++G** basis set[72], and single energy points were calculated at the MP2/6-311 ++G** level. All of the optimized structures were characterized to be true local energy minima on the potential energy surface without imaginary frequencies. Based on a Born–Haber energy cycle[66, 73] (Scheme 2), the heat of formation of a salt can be simplified by Equation (1):

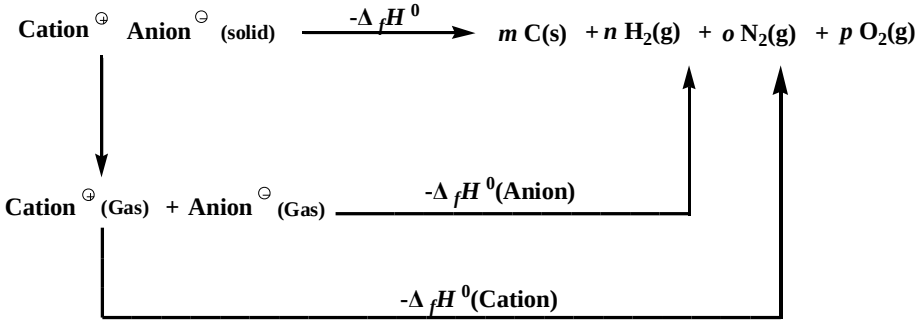

Scheme 2 Born–Haber cycle for the formation of energetic salts.

$$\Delta_f H^0(Salt, 298K) = \Delta_f H^0(Cation, 298K) + \Delta_f H^0(Anion, 298K) - \Delta H_L \quad (1)$$

where ΔH_L is the lattice energy of the ionic salts that could be predicted by Equation (2), as suggested by Jenkins et al.[74-76] as:

$$\Delta H_L = U_{POT} + [p(n_M/2-2) + q(n_X/2-2)]RT \quad (2)$$

where n_M and n_X depend on the nature of the ions M_p^+ and X_q^-, respectively, and are equal to 3 for monatomic ions, 5 for linear polyatomic ions, and 6 for nonlinear polyatomic ions. The lattice potential energy U_{POT} [Eq. (3)] can be calculated as follows:

$$U_{POT}/\text{kJ mol}^{-1} = \gamma(\rho_m / M_m)^{1/3} + \delta \quad (3)$$

where ρ_m [g/cm^3] is the density, M_m is the chemical formula mass of the ionic material, and values for δ and the coefficients γ [kJ/mol cm] and δ [kJ/mol] were taken from the literature[74-76].

The heats of formation of the cations and anions were computed by using the method of isodesmic reactions[77-79]. The isodesmic reaction for CA-anion is shown in Scheme 3 (isodesmic reactions for cations in Support Information). The enthalpy of the reaction, the scaled zero point energies, and other thermal factors are obtained. Thus, the detonation pressures (P) and detonation velocities (vD) were calculated by the empirical Kamlet–Jacobs equations (shown as Equation (4) and (5))[58, 76, 80, 81].

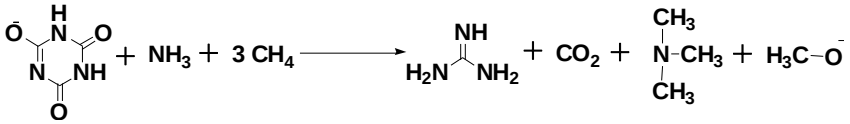

Scheme 3 Isodesmic reaction for calculating the heat of formation of the CA-anion.

$$D = 1.01(N\overline{M}^{1/2}Q^{1/2})^{1/2}(1+1.3\rho) \quad (4)$$

$$P = 1.558\rho^2 N\overline{M}^{1/2}Q^{1/2} \quad (5)$$

Where D is the detonation velocity (km/s), P is the detonation pressure (GPa), N is the explosive detonation that generated gas moles per gram (mol/g), $\overline{M}$ is the gaseous product of the average molecular weight (g/mol), Q is the explosive detonation chemical energy per gram (kJ/g), ρ is the density (g/cm). The Q value should be calculated first to calculate the D and P values. Q is also determined by the ΔH_f of the detonation reactant and product. Here, the parameters N, $\overline{M}$, and Q were calculated according to the chemical composition of each explosive[81] (shown in Table 4).

View Article Online
DOI: 10.1039/C5TA10688E

Table 4 Methods for Calculating the N, M and Q Parameters of the $C_aH_bO_cN_d$ Explosive

Parameter	Stoichiometric ratio		
	$c \geq 2a + b/2$	$2a + b/2 > c \geq b/2$	$b/2 > c$
N	$(b + 2c + 2d)/4M$	$(b + 2c + 2d)/4M$	$(b + d)/2M$
$\overline{M}$	$4M/(b + 2c + 2d)$	$(56d + 88c - 8b)/(b + 2c + 2d)$	$(2b + 28d + 32c)/(b + d)$
Q	$(28.9b + 94.05a + 0.239\Delta H_f^0)/M$	$[28.9b + 94.05(c/2 - b/4) + 0.239\Delta H_f^0)/M$	$(57.8c + 0.239\Delta H_f^0)/M$

$C_aH_bO_cN_d$ denotes the compound composed of the C, H, O, and N elements; *a, b, c,* and *d* stand for the number of C, H, O, and N atoms in the compound. N is moles of gaseous detonation products per gram of explosive (in mol/g); $\overline{M}$ is the average molecular weight of the gaseous products (in g/mol); Q is the chemical energy of detonation (in kJ/g); M in the formula is the molecular weight of the title compounds (in g/mol); ΔH_f^0 is the standard heat of formation of the studied compound (in kJ/mol).

General methods for characterization: FT-IR spectra was recorded on Nicolet 380 FT-IR spectrophotometer (Thermo Fisher Nicolet, USA) employing a KBr matrix with a resolution of 4 cm^{-1}, in the wavelength range of 400 cm^{-1} to 4000 cm^{-1}. The UV-vis spectra were measured using a UV-2102 PCS spectrophotometer with H_2O as the solution. ^1H NMR spectra was recorded with a JEOL GSX 600 MHz nuclear magnetic resonance (NMR) spectrometer. DMSO-*d*6 was a solvent and tetramethylsilane was an internal standard. Elemental analysis was performed on a Vario ELCUBE (Germany) Elemental Analyzer.

General method for the preparation of CA-anions salts and co crystal

Method for salts (sodium salt, barium salt, silver salt) based on CA

Sodium salt: NaOH (3.6 g, 90 mmol) was added to a suspension solution of CA (3.87 g, 30 mmol) in water (35 mL) with stirring until transparent solutions were formed. After remove the water under vacuum, the precipitate was filtered off, and washed three times with chilled ethanol (10 mL×3) to remove small amounts of NaOH. The product was then dried in a vacuum oven at 50 °C.

Barium salt: The solution of CA (1.29 g, 10 mmol, 250 mL H_2O) and $Ba(OH)_2$ $8H_2O$ (4.73 g, 15 mmol, 80 mL H_2O) were mixed with stirring at room temperature, and immediately precipitate appeared. The resulting suspension was stirred for another 2 h. Then, the precipitate was filtered off, and washed four times (ice-water, 5 mL×2; chilled ethanol 3 mL×2). The product was dried at 50 °C

Silver salt: In the dark condition, a solution of $AgNO_3$ (0.51 g, 3 mmol, 15 mL ethanol and 5 mL H_2O) was dropwise added to the suspension solution of CA (0.39 g, 30 mmol, 30 mL ethanol and 15 mL H_2O), and reflux for 1h. Then, the precipitate was filtered off, and washed four times (water, 5 mL×2; chilled ethanol 3 mL×2). The sliver salt was dried and stored in dark place.

Ammonium 4,6-dione-3,5-dihydro-[1,3,5]triazin-2-ol (1): CA (129 mg) was stirred in excess ammonia solution (15 mL) at room temperature for more than 24 h. The precipitate was filtered off, and washed several times with ice-water. Final product was freeze-dried to give a white powder (128 mg, 88% yield). UV-Vis (H_2O): λ_{max} = 215 nm; FT-IR (KBr) $\tilde{\nu}$: 3414, 3129, 2830, 1723, 1684, 1591, 1398, 1053, 777, 555; ^1H NMR (DMSO-*d*6, 600 MHz) δ: 7.68 (s, 4H, NH_4^+) pp; MS (ESI) *m/z*: 147.1 ($M + H^+$); Elemental analysis ($C_3H_6N_4O_3$, 146.04) Calcd: C 24.66%, H 4.14%, N 38.35%; Found: C 24.69%, H 4.35%, N 38.62%.

Hydrazinium 4,6-dione-3,5-dihydro-[1,3,5]triazin-2-ol (2): The same method was used as described for compound **2**, but by using hydrazine hydrate to give the product as white solid (145 mg, 90% yield). Salt **2** was recrystallized from water to get colorless crystalline solid. UV-Vis (H_2O): λ_{max} = 215 nm; FT-IR (KBr) $\tilde{\nu}$: 3451, 3295, 2828, 1716, 1594, 1484, 1356, 1133, 966, 782; ^1H NMR (DMSO-*d*6, 600 MHz) δ: 4.58 (s, 5H, $N_2H_5^+$) pp; MS (ESI) *m/z*: 162.1 ($M + H^+$); Elemental analysis ($C_3H_7N_5O_3$, 161.05) Calcd: C 22.36%, H 4.37%, N 43.47%; Found: C 22.10%, H 4.22%, N 43.25%.

Aminoguanidinium 4,6-dione-3,5-dihydro-[1,3,5]triazin-2-ol (3): A solution of aminoguanidine sulfate (123 mg, 1 mmol)

in water (5 mL) was added to a suspension solution of barium based on CA (200 mg) in water (30 mL) at room temperature with stirring overnight. The precipitate was filtered off, and the filtrate was retained. After removed the water under vacuum, white solid was washed four times (ice-water, 1.5 mL×2; chilled ethanol 1.5 mL×2). Product was dried in air to give a white powder (178 mg, yield 87.8%), which was recrystallized from distilled water to give colorless needles. UV-Vis (H_2O): λ_{max} = 214 nm; FT-IR (KBr) $\tilde{\nu}$: 3431, 2853, 1637, 1383, 1076, 779, 539; ^{1}H NMR(DMSO-*d*6, 600 MHz) δ: 4.61 (s, 2H,NH-NH_2), 6.54 (s, 4H, $H_2NCNH_2^+$), 7.63 (s, 1H, NH-NH_2), 9.32 (s, 2H, NH) pp; MS (ESI) *m/z*: 224.1 (M + H^+); Elemental analysis($C_4H_9N_7O_3$, 203.08) Calcd: C 23.65%, H 4.47%, N 48.26%; Found: C 23.69%, H 4.75%, N 48.42%.

Diaminoguanidinium 4,6-dione-3,5-dihydro-[1,3,5]triazin-2-ol (4): A solution of sodium based on CA(195 mg, 1 mmol) in water (2 mL) was added to a solution diaminoguanidinium hydrochloride (125 mg, 1 mmol) in water (1.5 mL). Then the addition was completed and precipitation appeared, and the resulting suspension was stirred for 2 h at room temperature. The resulting solid was collected by filtration and washed four times (ice-water, 1.5 mL×2; chilled ethanol 1.5 mL×2), and dried in air to give the desired product as a colorless crystalline solid (195 mg, yield 89.4%). UV-Vis (H_2O): λ_{max} = 215 nm; FT-IR (KBr) $\tilde{\nu}$: 3342, 3321, 3299, 3190, 2853, 1730, 1698, 1667, 1590, 1389, 1165, 1063, 983, 783, 555; ^{1}H NMR (DMSO-*d*6, 600 MHz) δ: 4.54 (s, 4H, NH-NH_2), 6.39 (s, 2H, CNH_2^+), 7.63 (s, 2H, NH-NH_2), 9.20 (s, 2H, NH) pp; MS (ESI) *m/z*: 219.2 (M + H^+); Elemental analysis ($C_4H_{10}N_8O_3$, 218.09) Calcd: C 22.02%, H 4.62%, N 51.36%; Found: C 22.00%, H 4.19%, N 51.45%.

Triaminoguanidinium 4,6-dione-3,5-dihydro-[1,3,5]triazin-2-ol (5): The same method was used as described for compound **4**. White solid (214 mg, yield 91.8%) was recrystallized from distilled water to give colorless needles. UV-Vis (H_2O): λ_{max} = 215 nm; FT-IR (KBr) $\tilde{\nu}$: 3535, 3449, 3320, 3212, 2836, 1747, 1656, 1601, 1486, 1386, 1334, 1127, 1086, 950, 783, 557; ^{1}H NMR (DMSO-*d*6, 600 MHz) δ: 4.47 (s, 9H, NH-NH_2), 9.18 (s, 2H, NH) pp; MS (ESI) *m/z*: 234.3 (M + H^+); Elemental analysis ($C_4H_{11}N_9O_3$, 233.1) Calcd: C 20.60%, H 4.72%, N 54.08%; Found: C 20.69%, H 3.75%, N 54.72%.

Aminonitroguanidinium 4,6-dione-3,5-dihydro-[1,3,5]triazin-2-ol (6): Aminonitroguanidine was prepared according to literature[82], and dissolved in concentrated hydrochloric acid. After standing at room temperature for two weeks, colorless cube crystal, aminonitroguanidinium hydrochloride, appeared. A solution of aminonitroguanidinium hydrochloride (156 mg, 1 mmol) in water (15 mL) was slowly added dropwise to a suspension solution of sliver salt based on CA (236mg) in water (30 mL) at room temperature with stirring overnight. After filtered precipitate, the filtrate was concentrated under vacuum, and the desired product as a colorless crystalline prism was filtered off. Thereafter, product dried in air (238 mg, yield 96.0%). UV-Vis (H_2O): λ_{max} = 212 nm, 267 (NO_2) nm; FT-IR (KBr) $\tilde{\nu}$: 3400, 3317, 3215, 1719, 1672, 1582, 1396, 1180, 1052, 777, 555; ^{1}H NMR (DMSO-*d*6, 600 MHz) δ: 4.68 (s, 2H, NH-NH_2), 7.56 (s, 2H, CNH_2^+), 8.30 (s, 1H, NH-NH_2), 9.28 (s, 2H, NH), 11.16 (s, 1H, NH-NO_2) pp; MS (ESI) *m/z*: 249.2 (M + H^+); Elemental analysis ($C_4H_8N_8O_5$, 248.06) Calcd: C 19.36%, H 3.25%, N 45.15%; Found: C 19.20%, H 3.19%, N 45.45%.

Aminocarbonylguanidinium 4,6-dione-3,5-dihydro-[1,3,5]triazin-2-ol (7): Compound **7** was get by the same method of salt **3**. White solid (218 mg, yield 94.3%). UV-Vis (H_2O): λ_{max} = 218; FT-IR (KBr) $\tilde{\nu}$: 3366, 3133, 2823, 1726, 1622, 1490, 1370, 1143, 1079, 776, 556; ^{1}H NMR (DMSO-*d*6, 600 MHz) δ: 6.29 (s, 2H, CNH_2), 7.20 (s, 2H, CNH_2^+), 7.65 (s, 2H, NH_2-C=O), 11.24 (s, 1H, NH-C=O) pp; MS (ESI) *m/z*: 232.1(M + H^+); Element analysis ($C_5H_9N_7O_4$, 231.07) Calcd: C 25.98%, H 3.92%, N42.41%; Found: C 25.77%, H 3.99%, N 42.45%.

Metforminium 4,6-dione-3,5-dihydro-[1,3,5]triazin-2-ol (8): According to the method of compound **6**. White solid (228 mg, yield 88.4%). UV-Vis (H_2O): λ_{max} = 221 nm; FT-IR (KBr) $\tilde{\nu}$: 3318, 3173, 3026, 2836, 1724, 1632, 1575, 1484, 1398, 1053, 780, 556; ^{1}H NMR (DMSO-*d*6, 600 MHz) δ: 2.92 (s, 6H, CH_3), 5.54 (s, 4H, $NH_2CNH_2^+$), 6.99 (s, 1H, NH=C), 7.68(s, 1H, C-NH-C), 9.55 (s, 2H, NH) pp; MS (ESI) *m/z*: 259.3 (M + H^+); Elemental analysis ($C_7H_{14}N_8O_3$, 258.12) Calcd: C 32.56%, H 5.46%, N 43.39%; Found: C 32.37%, H 5.99%, N 43.55%.

Co crystal of 5-amino-1*H*-tetrazole and cyanuric acid monohydrate (9): Product **9** was obtained by adding solution 5-amino-1*H*-tetrazole to a solution sodium based on CA (195 mg, 1 mmol). White solid (228 mg, yield 88.4%). UV-Vis (H_2O): λ_{max} = 214 nm; FT-IR (KBr) $\tilde{\nu}$: 3416, 2847, 1722, 1647, 1426,1295, 1072, 1055, 998; 828; 538; ^{1}H NMR (DMSO-*d*6, 600 MHz) δ: 9.40 (2H, NH) pp; MS (ESI) *m/z*: 215.2 (M + H^+); Elemental analysis ($C_4H_8N_8O_4$, 232.07) Calcd: C 20.69%, H 3.47%, N 48.27%; Found: C 20.95%, H 3.32%, N 49.54%.

Acknowledgments

We are grateful for financial support from the National Natural Science Foundation of China (51372211), Youth

Innovation Research Team of Sichuan for Carbon Nanomaterials (2011JTD0017), Open Project of State Key Laboratory Cultivation Base for Nonmetal Composites and Functional (project no. 14zdfk05), Southwest University of Science and Technology Outstanding Youth Fundation (project no. 13zx9107).

DOI: 10.1039/C5TA10688E

The authors are also expressed their appreciation to Xi'an Modern Chemistry Research Institute for help in impact sensitivities test.

References:

1. A. A. Dippold and T. M. Klapötke, *Chem.-Eur. J.*, 2012, **18**, 16742-16753.
2. C. Qi, S. H. Li, Y. C. Li, Y. Wang, X. K. Chen and S. P. Pang, *J. Mater. Chem.*, 2011, **21**, 3221.
3. S. Garg and J. M. Shreeve, *J. Mater. Chem.*, 2011, **21**, 4787.
4. G.H. Tao, B. Twamley and J. M. Shreeve, *J. Mater. Chem.*, 2009, **19**, 5850.
5. K. M. J. Crawford, T. M. Klapötke, F. A. Martin, C. M. Sabaté and M. Rusan, *Chem.-Eur. J.*, 2011, **17**, 1683-1695.
6. T. Abe, Y. H. Joo, G. H. Tao, B. Twamley and J. M. Shreeve, *Chem.-Eur. J.*, 2009, **15**, 4102-4110.
7. H. Gao, Y. Huang, C. Ye, B. Twamley and J. M. Shreeve, *Chem.-Eur. J.*, 2008, **14**, 5596-5603.
8. Y. G. Huang, Y. Q. Zhang and J. M. Shreeve, *Chem.-Eur. J.*, 2011, **17**, 1538-1546.
9. M. H. Huynh, M. A. Hiskey, E. L. Hartline, D. P. Montoya and R. Gilardi, *Angew. Chem. Int. Edit.*, 2004, **43**, 4924-4928.
10. C. Ye, H. Gao, J. A. Boatz, G. W. Drake, B. Twamley and J. M. Shreeve, *Angew. Chem. Int. Edit.*, 2006, **45**, 7262-7265.
11. M. H. V. Huynh, M. A. Hiskey, J. G. Archuleta and E. L. Roemer, *Angew. Chem. Int. Edit.*, 2005, **117**, 747-749.
12. T. M. Klapötke, A. Preimesser, S. Schedlbauer and J. Stierstorfer, *Cent. Eur. J. Energ Mat.*, 2013, **10**, 151-170.
13. H. Gao, R. Wang, B. Twamley, M. A. Hiskey and J. M. Shreeve, *Chem. Commun.*, 2006, **38**, 4007-40099.
14. D. E. Chavez, M. A. Hiskey and R. D. Gilardi, *Angew. Chem. Int. Edit.*, 2000, **112**, 1861-1863.
15. T. Wei, W. Zhu, J. Zhang and H. M. Xiao, *J. Hazard. Mater.*, 2010, **179**, 581-590.
16. X. Zhang, W. Zhu and H. M. Xiao, *Int. J. Quantum Chem.*, 2010, **110**, 1549-1558..
17. T. Wei, W. Zhu, X. W. Zhang, Y. F. Li and H. M. Xiao, *J. Phys. Chem. A*, 2009, **113**, 9404-9412.
18. M. B. Talawar, R. Sivabalan, T. Mukundan, H. Muthurajan, A. K. Sikder, B. R. Gandhe and A. S. Rao, *J. Hazard. Mater.*, 2009, **161**, 589-607.
19. X. J. Xu, H. M. Xiao, X. H. Ju, X. D. Gong and W. H. Zhu, *J. Phys. Chem. A*, 2006, **110** 5929-2933.
20. K. E. Gutowski, R. D. Rogers and D. A. Dixon, *J. Phys. Chem. A*, 2006, **110**, 11890-11897.
21. M. H. V. Huynh, M. A. Hiskey, D. E. Chavez, D. L. Naud and R. D. Gilardi, *J. Am. Chem. Soc.*, 2005, **127**, 12537-12543.
22. Q. L. Yan, T. Musil and S. Zeman, *Thermochimica Acta*, 2015, **604**, 106-114.
23. M. B. Talawar, R. Sivabalan, N. Senthilkumar, G. Prabhu and S. N. Asthana, *J. Hazard. Mater.*, 2004, **113**, 11-25.
24. H. Wei, C. He, J. Zhang and J. M. Shreeve, *Angew. Chem. Int. Edit.*, 2015, **54**, 9367-9371.
25. P. F. Pagoria, G. S. Lee, A. R. Mitchell and R. D. Schmidt, *Thermochimica Acta*, 2002, **384**, 187-204.
26. T. M. Klapötke, P. C. Schmid and S. Schnell, *J. Mater. Chem. A*, 2015, 119, 3509-3521.
27. A.I. Lesnikovich, O. A. Ivashkevich, S.V. Levchikl, A.I. Balabanovich, P.N. Gaponik and A.A. Kulak, *Thermochim Acta*, 2002, **388**, 233-251.
28. L. E. Fried, M. R. Manaa, P. F. Pagoria and R. L. Simpson, *Annu. Rev. Mater. Res.*, 2001, **31**, 291-321.
29. S.V. Levchik, A. I. Balabanovich, O.A. Ivashkevich, A.I. Lesnikovich, P.N. Gaponik and L. Costa, *Thermochimi Acta*, 1993, **225**, 53-65.
30. D. L. Strout, *J. Phys. Chem. A*, 2004, **108**, 10911-10916.
31. B. Klenke, M. P. Barrett, R. Brun and I. H. Gilbert, *J.Antimicrob. Chem.*, 2003, **52**, 290-293.
32. J. T. Sanderson, W. Seinen, J. P. Giesy and M. Berg, *Toxicol. Sci.*, 2000, **54**, 121-127.
33. L. Donald, Trepanier, K. L. Shriver and J. N. Eble, *J. Med. Chem.*, 1969, **12**, 257-260.
34. V. D. Ghule, S. Radhakrishnan, P. M. Jadhav and S. P. Tewari, *Chem.-Eur. J.*, 2012, **9**, 583-592.
35. H. M. LeBaron, H. Utah, J. E. McFarland, O. C. Burnside, et al, *Soil movement and persistence of triazine herbicides*, 2008.

36. D. Frem, *Combust. Explo., Shock+*, 2014, **50**, 441-446.
37. X. Q. Liang, Y. Zheng, B. Q. Wang and X. M. Pu, *Appl. Mech. Mater.*, 2013, **395-396**, 104-115.
38. F. Wang, H. Du, J. Zhang and X. Gong, *J. Phys. Chem. C*, 2012, **116**, 6745-6753.
39. M. H. Keshavarz, K. Esmailpoor and M. K. Tehrani, *Propell. Explos. Pyrot.*, 2010, **35**, 482-486.
40. K. Xu, D. M. Ho and R. A. Pascal, *J. Am. Chem. Soc.*, 1994, **116**, 105-110.
41. Y. C. Li, X. J. Zhang, G. Fu, S. P. Pang and C. L. Zhao, *Chin. J. Org. Chem.*, 2011, **31**, 1484-1489.
42. R. A. Henry, *J. Org.Chem.*, 1966, **31**, 1973-1974.
43. H. Gao and J. M. Shreeve, *Chem. Rev.*, 2011, **111**, 7377-7436.
44. Y. H. Joo and J. M. Shreeve, *J. Am. Chem. Soc.*, 2010, **132**, 15081-15090.
45. Y. H. Joo and J. M. Shreeve, *Angew. Chem. Int. Edit.*, 2010, **49**, 7320-7323.
46. T. T. Vo and J. M. Shreeve, *J. Mater. Chem. A*, 2015, **3**, 8756-8763.
47. T. M. Klapötke, P. C. Schmid and S. Schnell, *J. Mater. Chem. A*, 2015, **119**, 3509-3521.
48. V. Thottempudi, P. Yin, J. Zhang, D. A. Parrish and J. M. Shreeve, *Chem.-Eur. J.* , 2014, **20**, 542-548.
49. V. Thottempudi and J. M. Shreeve, *J. Am. Chem. Soc.*, 2011, **133**, 19982-19992.
50. Y. Zhang, Y. Guo, Y. H. Joo, D. A. Parrish and J. M. Shreeve, *Chem.-Eur. J.*, 2010, **16**, 10778-10784.
51. G. H. Tao, Y. Guo, D. A. Parrish and J. M. Shreeve, *J. Mater. Chem.*, 2010, **20**, 2999.
52. D. Fischer, T. M. Klapötke and J. Stierstorfer, *Angew. Chem.Int. Edit.*, 2015, **54**, 10299-10302.
53. Y. Guo, G. H. Tao, Y. H. Joo, R. Wang, B. Twamley, D. A. Parrish and J. M. Shreeve, *Energ. & Fuel.*, 2009, **23**, 4567-4574.
54. H. Wei, J.H. Zhang and J. M. Shreeve, *Chem.-Eur. J.*, 2015, **21**, 8607-8612.
55. H. G. Xue, B. Twamley and J. M. Shreeve, *Chem. Mater.*, 2007, **19**, 1731-1739.
56. J. Zhang and J. M. Shreeve, *J. Am. Chem. Soc.*, 2014, **136**, 4437-4445.
57. L. Liang, D. Cao, J. Song, H. Huang, K. Wang, C. Bian, X. Dong and Z. Zhou, *J. Mater. Chem. A*, 2013, **1**, 8857-8865.
58. D. Chand, D. A. Parrish and J. M. Shreeve, *J. Mater. Chem. A*, 2013, **1**, 15383.
59. V. Thottempudi, F. Forohor, D. A. Parrish and J. M. Shreeve, *Angew. Chem. Int. Edit.*, 2012, **51**, 9881-9885.
60. N. Fischer, D. Fischer, T. M. Klapötke, D. G. Piercey and J. Stierstorfer, *J. Mater. Chem.*, 2012, **22**, 20418.
61. J. T. Wu, J. G. Zhang, X. Yin, P. He and T. L. Zhang, *Eur. J. Inorg.Chem.*, 2014, **2014**, 4690-4695.
62. D. Fischer, T. M. Klapötke and J. Stierstorfer, *Propell. Explos. Pyrot.*, 2012, **37**, 156-166.
63. A. F. Holleman, E. Wiberg and N. Wiberg, *Lehrbuch der anorganischen Chemie, 102. Aufl., Walter de Gruyter, Berlin, New York,*, 2007.
64. Y. Tang, H. Gao, D. A. Parrish and J. M. Shreeve, *Chem.-Eur. J.* , 2015, **21**, 11401-11407.
65. K. E. Gutowski, R. D. Rogers and D. A. Dixon, *J. Phys. Chem. B*, 2007, **111**, 4788-4800.
66. H. Gao, C. Ye, C. M. Piekarski and J. M. Shreeve, *J. Phys. Chem. C*, 2007, **111**, 10718-10731.
67. M. W. Schmidt, M. S. Gordon and J. A. Boatz, *J. Phys. Chem. A*, 2005, **109**, 7285-7295.
68. N. Fischer, T. M. Klapötke, M. Reymann and J. Stierstorfer, *Eur. J. Inorg.Chem.*, 2013, **2013**, 2167-2180.
69. R. C. Crystal Structure 4.1: Crystal Structure Analysis Package, (2000-2014). Tokyo 196-8666, Japan.
70. G. M. SHELXL2014: Sheldrick, (2008). Acta Cryst. A64, 112-122.
71. M. Frisch, G. Trucks, H. Schlegel, G. Scuseria, M. Robb, J. Cheeseman, J. Montgomery J. T. Vreven, K. Kudin and J. Burant, *Gaussian Inc., Wallingford, CT*, 2004, 26.
72. R. G. Parr and W. Yang, *Density-functional theory of atoms and molecules*, Oxford university press, 1989.
73. V. D. Ghule, *J. Phys. Chem. C*, 2013, **117**, 16840-16849.
74. H. D. B. Jenkins, D. Tudela and L. Glasser, *Inorg. Chem.*, 2002, **41**, 2364-2367.
75. H. D. B. Jenkins, H. K. Roobottom, J. Passmore and L. Glasser, *Inorg. Chem.*, 1999, **38**, 3609-3620.
76. M. Sućeska, *Propell. Explos. Pyrot.*, 1991, **16**, 197-202.
77. M. Lu and G. Zhao, *J. Brazil. Chem. Soc.*, 2013, **24**, 1018-1026.
78. L. A. Curtiss, K. Raghavachari, P. C. Redfern, V. Rassolov and J. A. Pople, *J. Chem. Phys.*, 1998, **109**, 7764-7776.
79. L. A. Curtiss, K. Raghavachari, P. C. Redfern and J. A. Pople, *J. Chem. Phys.*, 1997, **106**, 1063-1079.
80. S. Bastea, L. Fried, K. Glaesemann, W. Howard, P. Souers and P. Vitello, *Lawrence Livermore National Laboratory*,

2007.
81. L. Qiu, H. Xiao, X. Gong, X. Ju and W. Zhu, *J. Mater. Chem.*, 2006, **110**, 3797-3807.
82. R. A. Henry, R. C. Makosky and G. Smith, *J. Am. Chem. Soc.*, 1951, **73**, 474-474.
83. Y. Q. Zhang, Y. G. Huang, D. A. Parrish and J. M. Shreeve, *J. Mater. Chem.*, 2011, **21**, 6891-6897.
84. R. H. Wang, H.Y. Xu, Y. Guo, R. J. Sa and J. M. Shreeve, *J. Am. Chem. Soc.*, 2010, **132**, 11904-11905.
85. W. Liu , Q. H. Lin, Y. Z. Yang, X. J. Zhang, Y. C. Li, Z. H. Lin and Pang, S. P. *Chem. Asian J*, 2014, **9**, 479-486.

View Article Online
DOI: 10.1039/C5TA10688E

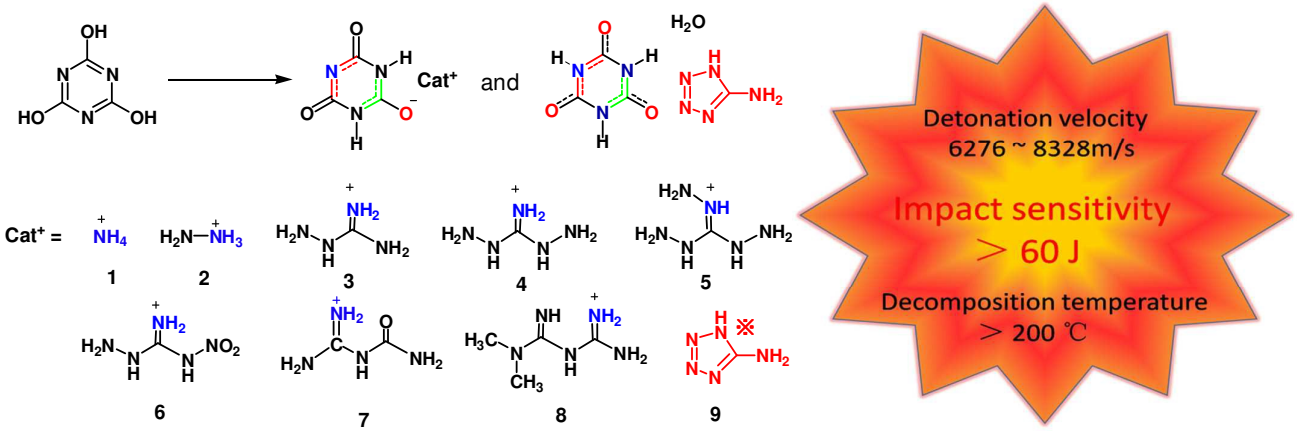

Graphical Abstract